Journal of proteome research

Article

pubs.acs.org/jpr

^{1}H NMR Global Metabolic Phenotyping of Acute Pancreatitis in the Emergency Unit

Alma Villaseñor,[†,‡] James M. Kinross,[*,§,†] Jia V. Li,[†] Nicholas Penney,[§] Richard H. Barton,[†] Jeremy K. Nicholson,[†] Ara Darzi,[§] Coral Barbas,[‡] and Elaine Holmes[*,†]

[†]Section of Biomolecular Medicine, Division of Computational and Systems Medicine, Department of Surgery and Cancer, Faculty of Medicine, Imperial College London, Sir Alexander Fleming Building, Exhibition Road, South Kensington, London SW7 2AZ, United Kingdom

[‡]Centre for Metabolomics and Bioanalysis (CEMBIO), Faculty of Pharmacy, Universidad San Pablo CEU, Campus Monteprincipe, Boadilla del Monte, 28668 Madrid, Spain

[§]Section of Biosurgery & Surgical Technology, Division of Surgery, Department of Surgery and Cancer, Faculty of Medicine, Imperial College London, QEQM Building, St. Mary's Hospital, London W2 1NY, United Kingdom

S *Supporting Information*

ABSTRACT: We have investigated the urinary and plasma metabolic phenotype of acute pancreatitis (AP) patients presenting to the emergency room at a single center London teaching hospital with acute abdominal pain using ^{1}H NMR spectroscopy and multivariate modeling. Patients were allocated to either the AP (n = 15) or non-AP patients group (all other causes of abdominal pain, n = 21) on the basis of the national guidelines. Patients were assessed for three clinical outcomes: (1) diagnosis of AP, (2) etiology of AP caused by alcohol consumption and cholelithiasis, and (3) AP severity based on the Glasgow score. Samples from AP patients were characterized by high levels of urinary ketone bodies, glucose, plasma choline and lipid, and relatively low levels of urinary hippurate, creatine and plasma-branched chain amino acids.

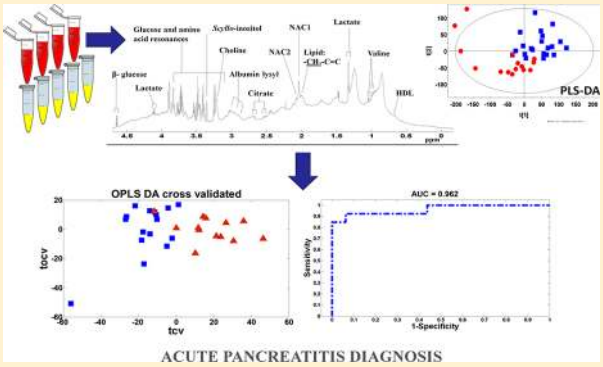

AP could be reliably identified with a high degree of sensitivity and specificity (OPLS-DA model R^2 = 0.76 and Q^2Y = 0.59) using panel of discriminatory biomarkers consisting of guanine, hippurate and creatine (urine), and valine, alanine and lipoproteins (plasma). Metabolic phenotyping was also able to distinguish between cholelithiasis and colonic inflammation among the heterogeneous non-AP group. This work has demonstrated that combinatorial biomarkers have a strong diagnostic and prognostic potential in AP with relevance to clinical decision making in the emergency unit.

KEYWORDS: *acute pancreatitis, abdominal pain, metabonomics, NMR, patient stratification*

INTRODUCTION

Acute pancreatitis (AP) is an inflammatory condition associated with a progressive systemic inflammatory response (SIRS) and, in severe cases, autonecrosis of pancreatic tissue, organ failure, and death.[1,2] In Europe, the mortality rate for this condition remains at 10%, and in severe cases associated with multiple organ failure it can be as high as 30%. AP affects between 5 and 80/100 000 people globally, and the mainstay of therapy in the acute phase is the rapid initiation of supportive treatments, the treatment of reversible underlying causes, and the allocation of intensive therapies, where needed. In the U.K., an AP diagnosis is conventionally made on patient history, clinical examination, and the measurement of serum amylase. However, this lacks sensitivity and specificity, and it is subject to variation in its diagnostic threshold over time after the initial pancreatic insult.[3] Although other biomarkers are available (e.g., serum pancreatic lipase or urinary amylase), they do not provide prognostic value and they are expensive. Imaging modalities such as ultrasound (USS) and dynamic computed tomography (CT) scanning may also be used to confirm the diagnosis of AP;[4] however, USS is nonspecific and a CT is only used to assess severity at 72 h or to rule out other diagnoses. Prognostication is essential in AP for early organ support and minimization of mortality. Unfortunately, clinical risk scores such as the Glasgow score,[5] are only marginally more accurate than clinical intuition.[6−10] Other generic physiological scoring systems are used in critical care such as the Acute Physiology and Chronic Health Evaluation (APACHE II) score,[11] a generic physiological measurement based on 12 parameters, that is designed to measure the severity of disease for adult patients 24 hrs following admission to intensive care units. However, this is not disease-specific for AP. Ultimately, diagnosing the etiology of the underlying condition remains the only methodology for

Received: February 19, 2014

   dx.doi.org/10.1021/pr500161w | *J. Proteome Res.* XXXX, XXX, XXX−XXX

preventing disease progression and further episodes of AP. Although alcohol consumption and cholelithiasis are responsible in 60−80% of cases of AP,[12,13] the causes are multiple, and 10% of cases are classed as idiopathic, severely limiting definitive therapeutic options in this cohort of patients.

Metabolic profiling coupled to computational modeling has emerged as a tool for describing metabolic systems and is capable of characterizing different time points in diseases.[14−16] The determination of metabolite changes that describe a biological phenotype based on either ^{1}H nuclear magnetic resonance (NMR) spectroscopy or mass spectrometry (MS) has been widely applied for global profiling to define diagnostic or prognostic biofluid profiles for physiological or pathological states.[14,17−19] However, to demonstrate that a metabonomic strategy for characterizing pathology has genuine translational capacity, it must be robust enough to cope with the complex clinical heterogeneity encountered in real-world clinical environments such as the emergency room, which differ greatly from standardized and tightly controlled experimental environments. To our knowledge, this approach has yet to be prospectively applied to patients with AP presenting in the acute setting, although a small NMR-based comparison has been made between AP patients from an inpatient clinic (n = 5) with healthy controls from an outpatient (n = 5).[20] A key feature of AP is abdominal pain, a common and often nonspecific presenting complaint for a large array of other surgical pathologies that require urgent treatment. However, 40% of all cases of acute abdominal pain are labeled, as being "nonspecific". The aim of the current study was therefore to determine the potential of a metabonomic approach in the diagnosis and prognostic staging of AP and to ascertain the clinical utility of this approach in the analysis of acute abdominal pain in the emergency setting.

MATERIALS AND METHODS

Study Design

This was an observational control study of consecutive patients presenting with acute abdominal pain to a single center "Accident and Emergency" unit at St. Mary's hospital, London, U.K. All work was approved the by the ethical committee in St. Mary's Hospital, London (Rec 05/Q0403/201). The inclusion criteria were designed to be pragmatic. Therefore, patients were included if they presented with acute severe abdominal pain of <72 h duration or if they demonstrated signs of peritonitis when examined by the emergency physician on their first examination. Patients were excluded if they had been discharged from hospital within 72 h with the same pain, if they were unconscious at presentation, if they were pregnant, if they were under the age of 18, or if they had undergone surgery within the previous 6 weeks or received a blood transfusion. Patients with congenital pancreatic malformations or those with cystic fibrosis were also excluded. Patients with AP were identified by their medical history and examination and an elevated amylase that was greater than three times the standard range (0−90 units/L). A pancreatic lipase assay was not routinely available for use within the hospital. Patients were investigated and managed as per the current British Society of Gastroenterology guidelines.[21] Therefore, all patients underwent an abdominal ultrasound (USS) within 24 hrs and a CT of the abdomen at 72 hrs if no clinical improvement was obtained or sooner if clinically indicated. Patients underwent clinical severity scoring using the modified Glasgow criteria[5] at 24 and 48 hrs. All patients were given a diagnosis for their etiology, and underwent an endoscopic retrograde cholangiopancreatography (ERCP) on the same admission if evidence of obstructive biliary cholelithiasis was demonstrated. Patients with a previous history of pancreatitis (i.e., > 2 episodes) were subcategorized to have either recurrent or acute chronic pancreatitis (CP). CP has a different mechanism and clinical presentation,[22] and these patients were therefore excluded from the final analysis. The clinical diagnosis on discharge from hospital was used for patient phenotyping, as determined by the attending consultant physician. The aim was to achieve a practical representation of how clinical, biochemical, and imaging data can be used to reach the diagnosis during the admission phase and to determine if a metabonomic method was able to augment this approach and to differentiate patients or subsets of patients according to presence, severity, or cause of AP in an early stage. The 30 day follow-up data were also recorded to confirm the final diagnosis. The non-AP patients group was investigated according to the discretion of the attending surgeon. However, their diagnosis was confirmed on the basis of the clinical presentation, basic serum, and urine biochemistry and on imaging by USS or CT or at the time of surgery with histopathological analysis. All patients had clinical observation data (pulse, temperature, and blood pressure) and routine clinical biochemical data collected on admission and then at 24 h intervals until the patient underwent surgery or was discharged. Samples were collected from each patient for the first 5 days of their admission. Samples for metabonomic analysis were collected as soon as possible after attendance of the patient in the emergency room or within 24 hrs of admission to hospital. Patients not recruited prior to this cutoff were excluded.

Sample Collection and Preparation

Urine Samples. Sampling was performed precatheterization wherever possible. If catheterized, a "clean catch" sample was taken. Urine samples were kept on ice after collection prior to being stored frozen at −80 °C. Urine samples were thawed on ice, vortexed, and centrifuged; they were prepared by adding 200 μL of phosphate buffer pH 7.4 containing 20% of D_2O to 400 μL of urine. The mixture was transferred into a 5 mm outer diameter NMR tube. All ^{1}H NMR spectra were acquired using a Bruker DRX600 spectrometer (Rheinstetten, Germany) with a 5 mm TXI probe operating at 600.13 MHz. The field frequency was locked on to D_2O solvent. Primary acquisitions were made using a standard 1-D pulse program [recycle delay (RD)-90°-t_1-90°-t_m-90°-acquire free induction decay (FID)]. The 90° pulse length was adjusted to ∼12 μs. A total of 64 scans were recorded into 32 K data points with a spectral width of 20 ppm at 300 K. An exponential function was applied to the FID prior to the Fourier transformation, which resulted in a line broadening of 0.3 Hz.

Plasma Samples. Plasma samples were collected in 5 mL aliquots and in heparinized lithium tubes, and they were kept on ice before being centrifuged. The supernatant obtained was frozen at −20 °C until the day of analysis. 200 μL of plasma was added to 400 μL of 0.9% saline solution containing 10% of D_2O. ^{1}H NMR spectra of the plasma samples were acquired employing two 1-D NMR experiments. These were a standard 1-D pulse sequence (as described for urine) and a Carr−Purcell−Meiboom−Gill (CPMG) pulse sequence [RD-90°-(τ-180°-τ)$_n$-acquire FID] giving a total spin−spin relaxation delay ($2_n\tau$) of 80 ms, determined by the number of spin echoes and τ

dx.doi.org/10.1021/pr500161w | J. Proteome Res. XXXX, XXX, XXX−XXX

Table 1. Summary of Clinical Data

		non-AP (n = 23)	pancreatitis (n = 15)	p value
age (median, range)		42 (18−77)	50 (22−70)	0.980
sex	F:M	12:11	3:12	0.001
	cholecystitis	1		
	biliary colic	1		
	ascending cholangitis	1		
	appendicitis	5		
	diverticulitis	3		
	colitis	2		
	adhesions	1		
	unknown	2		
	UTI	3		
	renal colic	1		
	cecal volvulus	1		
	gastritis	1		
	mumps orchitis	1		
	gall stone pancreatitis		6	
	EtOH pancreatitis		9	
amylase (mean, SD)		62.1 (73.7)	874.6 (841.8)	1.3×10^{-06}
symptom duration (mean, SD)		33.4 (24.1)	41.9 (23.8)	0.860
Glasgow 24 h (mean, SD)		0	2.1 (1.8)	
Glasgow 48 h		0	1.1 (1.3)	
APACHE 24 h (mean, SD)		3.3 (3.2)	9.6 (6.3)	0.014
APACHE 48 h		1.9 (3.0)	5.8 (3.9)	0.140
length of stay, days (median, range)		3 (0−14)	7 (2−132)	0.020

[a]Data presented is the average (range or SD). Data were analyzed by unpaired two-tailed Student's t test.

= 400 μs. Typically, in the standard 1-D and CPMG experiments, 256 and 128 transients were collected into 32 k data points, respectively, at 300 K. All method characteristics and details are detailed elsewhere.[23]

Data Processing of NMR Spectra. All urine and plasma NMR spectra were automatically phased, baseline-corrected, and referenced to either sodium 3-(trimethylsilyl) propionate-2,2,3,3-d_4 (TSP; δ 0.0) or α-glucose (δ 5.23) for urine and plasma, respectively, using in-house scripts. The spectra were imported to Matlab and the region containing water and urea resonances (δ 4.7 to 6.2) and TSP (δ −0.1 to 0.1 for urinary spectra only) were removed. Peak alignment[24] and spectral normalization using a probabilistic quotient algorithm[25] were performed in the full-resolution spectra using an in-house Matlab script (The MathWorks, Natick, MA).

Multivariate Analysis. Principal component analysis (PCA) was applied to NMR spectral data sets to visualize outliers and data trends.[26] Partial least-squares discriminant analysis (PLS-DA) was performed to optimize the classification of samples and aid identification of candidate biomarkers associated with clinical phenotype. Orthogonal-PLS-DA (OPLS-DA)[27] was also carried out to optimize recovery of potential biomarkers, that is, compounds with high correlation and covariance with the class (e.g., disease severity or etiology). Modeling was conducted in SIMCA-P v.12.1 using unit variance scaling. Pseudoloadings plots were created with a color code projected onto the spectrum[28] to indicate the correlation of the metabolites discriminating between the classes in each comparison, that is, representing AP and other abdominal pain etiologies. Red indicates high correlation and dark blue denotes no correlation with sample class. The direction and magnitude of the signals relate to the covariance of the metabolites with the class in the model. The quality of the models was assessed by the cumulative R^2 and Q^2, indicating the goodness of fit and the predictive power of each model using SIMCA software (Umetrics SIMCA-P+12.0.1 software). Metabolite identification was based on chemical shifts published in literature and statistical total correlation spectroscopy (STOCSY) of peaks[29] (e.g., STOCSY of urinary 3-hydroxyisovalerate is shown in Supplemental Figure 1, SI). HMDB[30] and COLMAR[31] online databases were also used to confirm the chemical shift values for all metabolites. Finally, where unknown metabolites were identified or there was uncertainty in the metabolite identity, 2D NMR experiments, for example, ^{1}H−^{1}H total correlation spectroscopy (TOCSY), ^{1}H−^{13}C heteronuclear multiple quantum coherence (HMQC), and heteronuclear single quantum coherence (HSQC), were performed for complete chemical structure elucidation. Parametric clinical data were analyzed by unpaired two-tailed Student's t test using SPSS v.19.0.

Exclusion of Outliers and Sample Processing. A total of 46 patients were enrolled into the study (AP = 22, non-AP = 24). From this initial recruitment, five patients had chronic pancreatitis (CP) and were excluded; an example of urinary CP spectrum is shown in Supplemental Figure 2, SI. Additionally, strong outliers detected either by extremely unusual NMR spectra dominated by a few signals or by significant broadened signals due to, for example, excess proteinuria were removed. Finally, after removing the patients unable to provide samples, the numbers of patients for urine analysis were AP = 13 and non-AP = 18, while those for plasma were AP = 15 and non-AP = 21.

RESULTS

Clinical Data

Patients were aged 18 to 77 years old, with a median age of 42.5 years (SD = 16.8). The remaining demographic data are

dx.doi.org/10.1021/pr500161w | J. Proteome Res. XXXX, XXX, XXX−XXX

provided in Table 1. The etiologies of pain in the non-AP patients group were heterogeneous, reflecting the typical distribution of the causes of acute abdominal pain presenting to a typical accident and emergency department[32] (Table 1). Two patients in this cohort were not given a definitive diagnosis for their abdominal pain, and three patients had a primary biliary pathology but with a normal blood amylase level at presentation. The etiologies of the AP group were due to either cholelithiasis (6/15) or alcohol (9/15). One of the cholelithiasis AP cohorts had necrotic pancreatitis. The mean Glasgow score (a disease-specific clinical risk score of severity ranging between 0 and 3, where 3 represents a severe episode) was 2.07 at 24 h and 1.07 at 48 h, indicating that this cohort of AP suffered moderately severe episodes. However, one patient with cholelithiasis AP and one patient with alcoholic AP diagnosis had a myocardial infarction during their admission, both of whom were treated with a standard acute coronary syndrome protocol. The APACHE II score[11] varied significantly between the groups, indicating the increased general severity of illness in the AP group compared with the non-AP group. This was also reflected in the hospital length of stay data, which differed significantly (average for non-AP group = 3 and AP = 7; $p < 0.02$) between diagnostic groups (Table 1).

Characterizing the Urinary Phenotype of AP

The urinary ^{1}H NMR spectra from this clinical study demonstrated substantial interindividual variation. Figure 1, shows urinary ^{1}H NMR spectra from an alcoholic AP patient (A) and a non-AP patient (B). In general, spectra from AP patients were characterized by high concentrations of urinary glucose and ketone bodies. Unsurprisingly, large concentrations of acetate, ethanol, acetone, and ethyl glucuronide were also observed in this patient, reflecting the underlying etiology (Figure 1A). Ethanol was not consistently observed in the six patients with alcohol-induced pancreatitis due to the varying volume of alcohol consumed between patients and time since ingestion (range 24 h to 1 week). Furthermore, it was apparent from visual inspection across both groups (AP and non-AP) of urinary spectra that metabolites from common analgesic nonsteroidal anti-inflammatory drugs (such as ibuprofen) were observed (data not shown), as might be expected in a cohort of patients presenting with abdominal pain. Signals from the drug acetaminophen metabolites were present in both groups, but they varied between patients; higher concentrations of acetaminophen metabolites can be observed in the cholecystitis sample in Figure 1B. NMR spectral profiles of acetaminophen and ibuprofen and their urinary metabolites have been published previously.[33,34] Urine specimens from several patients contained high concentrations of mannitol [δ 3.65(dd); δ 3.73(m); δ 3.77(d); δ 3.84(dd)] used as an excipient in the acetaminophen preparation and which was therefore correlated with acetaminophen and its related urinary metabolites [acetaminophen sulfate (AS) = δ 2.18(s), δ 7.31(d), δ 7.46(d); acetaminophen glucuronide (AG) = δ 2.17(s), δ 3.62(m), δ 5.10(d), δ 7.13(d), δ 7.36(d); acetaminophen (A) = δ 2.16(s), δ 6.91(d), δ 7.25(d); *N*-acetylcysteine conjugate (NAC) = δ 1.86(s)]. The drug-related origin of the mannitol was supported by a Pearson correlation test[35] using all compounds in the profile and a selected driver peak for the mannitol signal (δ 3.805 ppm, (5-CH)), with an established cutoff of $p < 0.05$. The resulting graph showed mannitol signals and acetaminophen (A, AG, AS, and NAC) was positively and highly correlated, showing correlations values above 0.897 (from NAC 6.98(d)) with a p value of 0.039 (Supplemental Figure 3, SI). This relationship was confirmed by ^{1}H NMR analysis of the intravenous acetaminophen preparation, a common analgesic given in the acute setting and by correlation with the patient drug charts that demonstrated the drug was given in the emergency room. Mannitol is a commonly used excipient in acetaminophen formulations.[36] The regions containing mannitol (from δ 3.65 to δ 3.97) and acetaminophen metabolites (from δ 1.85 to δ 1.88; δ 2.14 to δ 2.2; δ 3.59 to δ 3.65; δ 7.11 to δ 7.18; and δ 7.29 to δ 7.49) were therefore removed from the raw data for the remaining analysis to minimize any confounding effects unrelated to the disease etiology or severity.

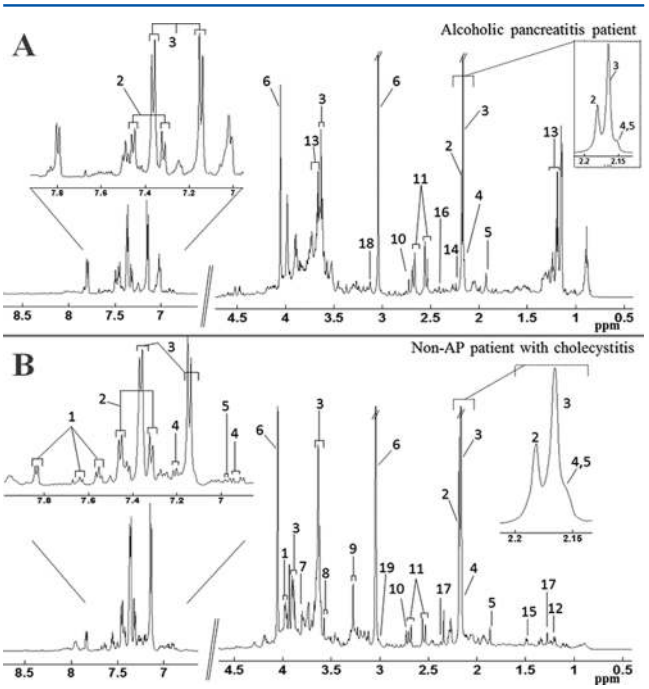

Figure 1. Typical 600 MHz ^{1}H NMR spectra of urine obtained from a patient with acute pancreatitis and alcoholic background (A) and a non-AP patient with cholecystitis (B). Sections from the NMR spectra (raw data) show the metabolite differences describing the physical condition. Key: 1, hippurate; 2, acetaminophen sulfate (AS); 3, acetaminophen glucuronide (AG); 4, acetaminophen (A); 5, *N*-acetylcysteine conjugate of acetaminophen (NAC); 6, creatinine; 7, guanidinoacetate; 8, glycine; 9, trimethylamine-*N*-oxide (TMAO); 10, dimethylamine; 11, citrate; 12, D-3-hydroxybutyrate; 13, ethanol; 14, acetone; 15, alanine; 16, succinate; 17, 3-hydroxyisovalerate; 18, malonic acid; 19, creatine.

Plasma NMR Spectra

There were few obvious disease-specific metabolites that varied systematically between raw spectra; however, clear quantitative changes in the spectra were observed, particularly in concentrations of VLDL, LDL, and nonesterified fatty acids. A comparison of 1-D NMR spectra from an AP and a non-AP patient with appendicitis is shown in Figure 2, illustrating the gross differences in the lipoproteins. Likewise, a comparison of CPMG raw spectra from different patients, an AP and non-AP patient diagnosed with diverticulitis, is presented in Figure 4 in the SI, where differences of VLDL were observed.

dx.doi.org/10.1021/pr500161w | J. Proteome Res. XXXX, XXX, XXX–XXX

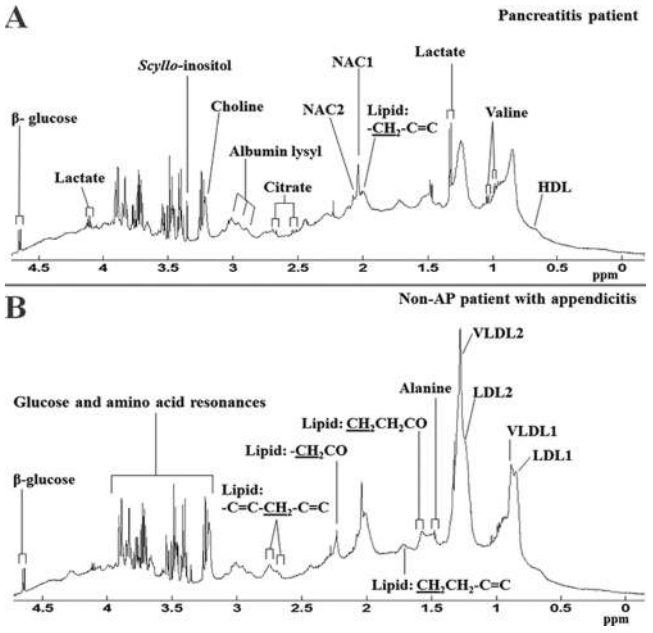

Figure 2. 600 MHz ^{1}H NMR spectra (δ −0.0 to 4.7) of plasma from (A) pancreatitis patient and (B) non-AP patient diagnosed with appendicitis. Abbreviations: LDL1 and VLDL1 refer to the terminal CH_3 groups of fatty acids in low-density and very-low-density lipoproteins, respectively. HDL refers to the C18 signal from cholesterol in high-density lipoprotein. NAC1 and NAC2 refer to composite acetyl signals from α1-acid glycoprotein.

Multivariate Modeling of Patients with Severe Abdominal Pain

Three main analyses were performed based on clinical criteria: (1) diagnosis of AP (AP vs non-AP), (2) etiology (alcohol consumption vs cholelithiasis), and (3) AP severity, based on a validated modified Glasgow score comparison of mild (Glasgow score 1) versus moderate to severe (Glasgow score 2 and 3). It was not possible to build predictive models for organ failure or mortality based on the small numbers of patients. PCA, PLS-DA, and OPLS-DA models were therefore created to determine the capacity of the metabolic profiles to classify the sample set according to the above outcomes and to determine how well the model could predict the class of samples according to the principal diagnosis. PCA models did not show clear separation for any of the clinical scenarios in this study due to the extreme heterogeneity of the data. PLS-DA plots for each clinical scenario in urine and plasma (CPMG- and 1-D-spectral) data (Figure 3) showed positive predictive models for all with the exception of prediction of etiology in the plasma (1-D-plasma and CPMG) data set. Discriminatory metabolites were found in the OPLS-DA pseudoloading plots for each of the three sets of models for AP prediction, severity, and etiology in urine and plasma (Figure 4) and differed in composition between models assessing different outcomes. Discriminant metabolites found in plasma and urine for the three clinical scenarios are summarized in Tables 2−4 and discussed below.

1. Diagnosis. Consistent changes in concentrations of urinary and plasma metabolites were found between the AP and the non-AP group. Plasma acetone, D-3-hydroxybutyrate, acetoacetate, glucose, lipid signals (CH_3CH_2−, CH_2CH═CH) fraction, and plasma choline concentrations were increased in AP patients. Low urinary levels of hippurate, creatine, and plasma valine and alanine were also characteristic of the AP group (Table 2). Because hippurate is a well-established gut microbial cometabolite derived from glycine conjugation of benzoic acid,[37,38] a subgroup analysis of antibiotic-treated patients (n = 10; 5non-AP/5AP) and non-antibiotic-treated (n = 21; 12non-AP/9AP) patients was performed to determine if antibiotic ingestion in the AP diagnostic model was responsible for the difference in urinary excretion of hippurate between the two groups (Figure 5 and Supplemental Table 1, SI). The PLS-DA analysis demonstrated class separation according to antiobiotic usage (R^2 = 0.85, Q^2 = 0.47) based on modulation of a combination of metabolites including decreased urinary citrate, methylamine, and creatinine, suggesting that antibiotic use did have a systemic metabolic impact in this group of patients. Some of the differentiating signals derived directly from antibiotics (e.g., metronidazole[39]). Concentrations of 3-hydroxyisovaleric acid previously reported to be a gut microbial cometabolite[40] were decreased in the antibiotic group. However, hippurate concentrations did not vary significantly (driver peak = δ^1H 7.85 (6-CH); correlation (r) = −0.29; p = 0.11) between groups, suggesting that the AP pathophysiology has a greater effect on this mammalian-host cometabolite than antibiotic use. In addition to signals from analgesics and NSAID metabolites (Figure 5, SI), the multivariate urinary model of antibiotic usage (Figure 5 and Supplemental Table 1, SI) shows unknown compounds whose excretion was increased in the antibiotic group, which are most likely to be xenometabolites. Antibiotic usage was associated with decreased urinary concentrations of 3-hydroxyisovalerate, methylamine, citrate, and creatinine.

To compare the robustness of the metabonomic models in urine and plasma, we created receiver operating characteristic (ROC) curves (Figure 6A,B). The urine ^{1}H NMR model (AUC = 0.91) produced a stronger diagnostic model than plasma (AUC = 0.86). The urinary multivariate model had a high sensitivity with true-positive rates (TPRs) of 0.5 to 0.6, low false-positive rates (FPR) of <0.2, and a classification rate of ≥80%. Additionally, 10 metabolites (5 from each biofluid) were combined to generate a definitive diagnostic ROC curve (Figure 6C). This demonstrated a stronger diagnostic model for AP (AUC = 0.96) when compared with each biofluid separately. Moreover, to emphasize the quality of the differential biomarker for the diagnosis, a PCA analysis was performed based on these 10 discriminant metabolites. The scores plot (Supplemental Figure 6A, SI) showed a clear separation of disease groups. The permutation test (Figure 6B, SI) for these metabolites indicated that the model was robust. Moreover, the cross-validated OPLS-DA was also more robust (Figure 6D, R^2 = 0.76, Q^2 = 0.59). Serum amylase data had a sensitivity of 100% and a specificity of 95%, which although comparable to the metabonomic data is likely to be of little significance, as it was used as a diagnostic criterion and it had no prognostic value.

2. Etiology. Multivariate models of alcohol versus cholelithiasis AP had a good classification capacity (R^2Y from 51 to 90%) but variable predictive capacity; Q^2 ranged from 0 to 24% (Figure 3(ii)). The models generated from the plasma (CPMG and 1-D) spectra carried a negative predictive value in the first component, indicating that there was no clear diagnostic signature for etiology based on the low-molecular-weight components in plasma. However, OPLS-DA from urinary ^{1}H NMR spectra generated a stronger model (R^2Y = 0.76, Q^2 = 0.44), confirming that urinary ketone body excretion

dx.doi.org/10.1021/pr500161w | J. Proteome Res. XXXX, XXX, XXX−XXX

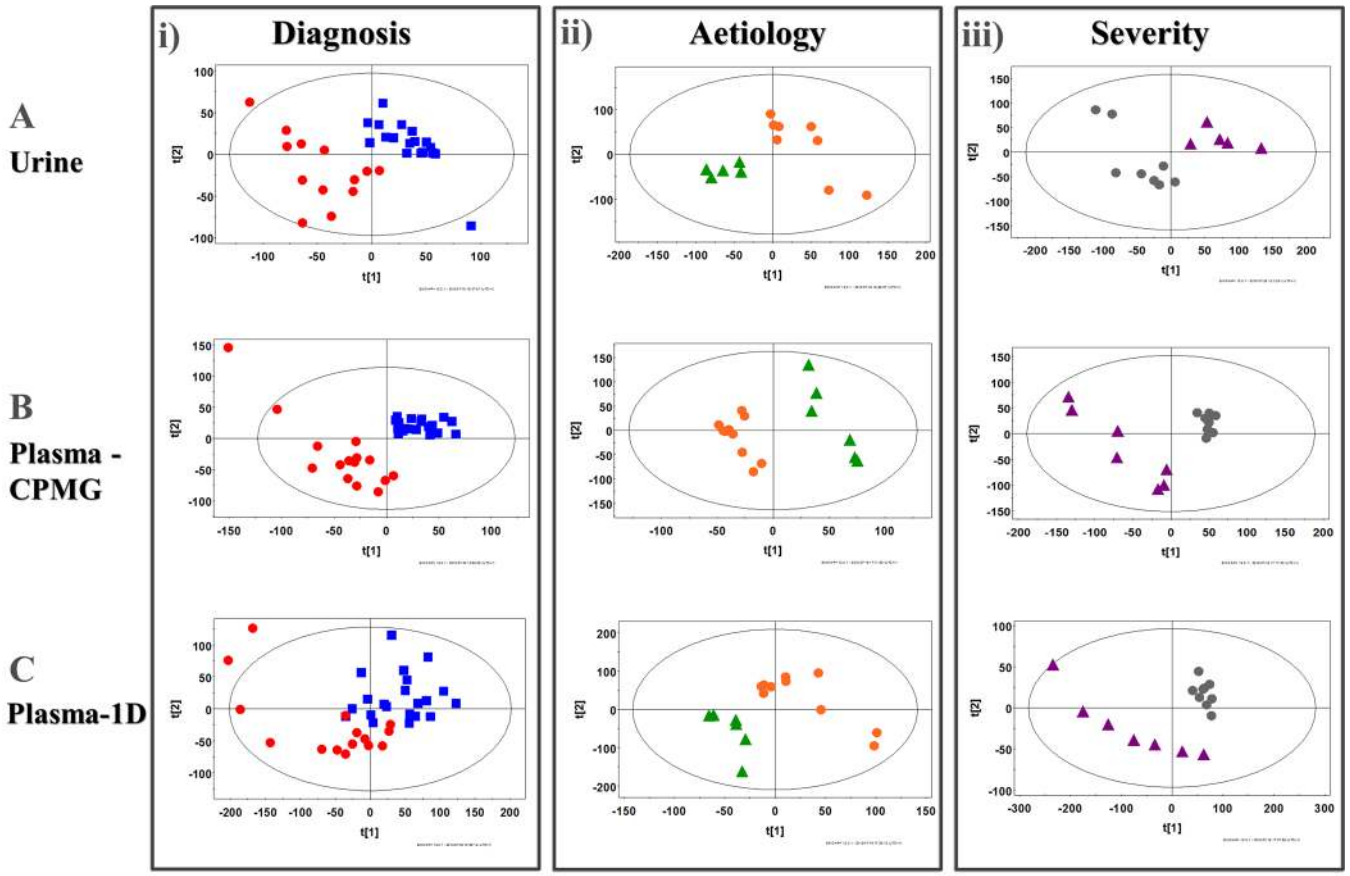

	Diagnosis		Aetiology		Severity	
	R^2	Q^2	R^2	Q^2	R^2	Q^2
Urine	0.84	0.35	0.90	0.24	0.87	0.36
CPMG	0.89	0.55	0.88*	-0.10*	0.96	0.64
1D-Plasma	0.59	0.26	0.51*	-0.10*	0.92	0.33

Figure 3. Scores plot of the first versus second component for partial least-squares discriminant analysis for (A) urine, (B) plasma-CPMG, and (C) 1-D-plasma for three different comparisons: (i) AP versus non-AP (diagnosis); (ii) etiology of AP patients, alcoholic versus cholelithiasis background; and (iii) severity of AP group based on Glasgow score, mild AP severity (Glasgow 1) versus moderate to severe AP (Glasgow 2−3). Key: *, value for the first component only, unit variance scaling; two principal components; R^2 and Q^2 values indicate variance explained and predictivity of the model respectively. (i) ●, AP samples (An = 13, B-Cn = 15); ■, non-AP samples (An = 18, B-Cn = 21). (ii) ●, Alcoholic AP samples (An = 8, B-Cn = 10); △, cholelithiasis AP samples (An = 5, B-Cn = 6). (iii) ●, Glasgow 1 group (An = 8, B-Cn = 9); △, Glasgow scores 2 and 3 group (An = 5, B-Cn = 7).

of acetone, acetatoacetate, and urinary 3-hydroxyisovalerate is of importance in the diagnosis of alcoholic AP compared with AP patients with cholelithiasis (Table 3; Figure 4C,(i)). The rest of metabolites from the plasma models (glucose and D-3-hydroxybutyrate) were discarded from the analysis (Figure 4B,C,(ii)).

3. Severity of AP. Multivariate models for disease severity were created using the Glasgow score as a surrogate marker. Both plasma and urine produced robust predictive models, but plasma CPMG data generated the strongest model ($R^2Y = 0.96$, $Q^2 = 0.64$), with tight clustering of those AP patients with mild disease, indicating that it was the low-molecular-weight components of plasma that were modulated most according to disease severity. Plasma metabolites such as creatinine, alanine, valine, choline, and *N*-acetyl signals from α1-acid glycoprotein were inversely related to disease severity, while increased plasma glucose strongly correlated with severity (Table 4, Figure 4(iii)). Of note, in patients with more severe disease, it was also possible to detect biomarkers of plasma expanders (such as the colloid "volplex"), which are commonly used to resuscitate patients with hypovolaemic or septic shock. However, the removal of these treatment-related resonances from the models did not impact the model quality or endogenous correlates with disease severity.

Finally, for non-AP group data analysis, patients were divided in two principal cohorts: those with (A) cholelithiasis and (B) colonic inflammation, that is, patients with diverticulitis, appendicitis, Crohn's disease, and intestinal ischemia. Patients that did not fit the defined criteria for either of cholelithiasis or colonic inflammation group were excluded for the comparison (e.g., patients with urosepsis or nonspecific abdominal pain without a diagnosis). Robust PLS-DA models for urine and plasma indicated that the cholelithiasis subgroup was metabolically distinct from the colonic inflammation subgroup

dx.doi.org/10.1021/pr500161w | J. Proteome Res. XXXX, XXX, XXX−XXX

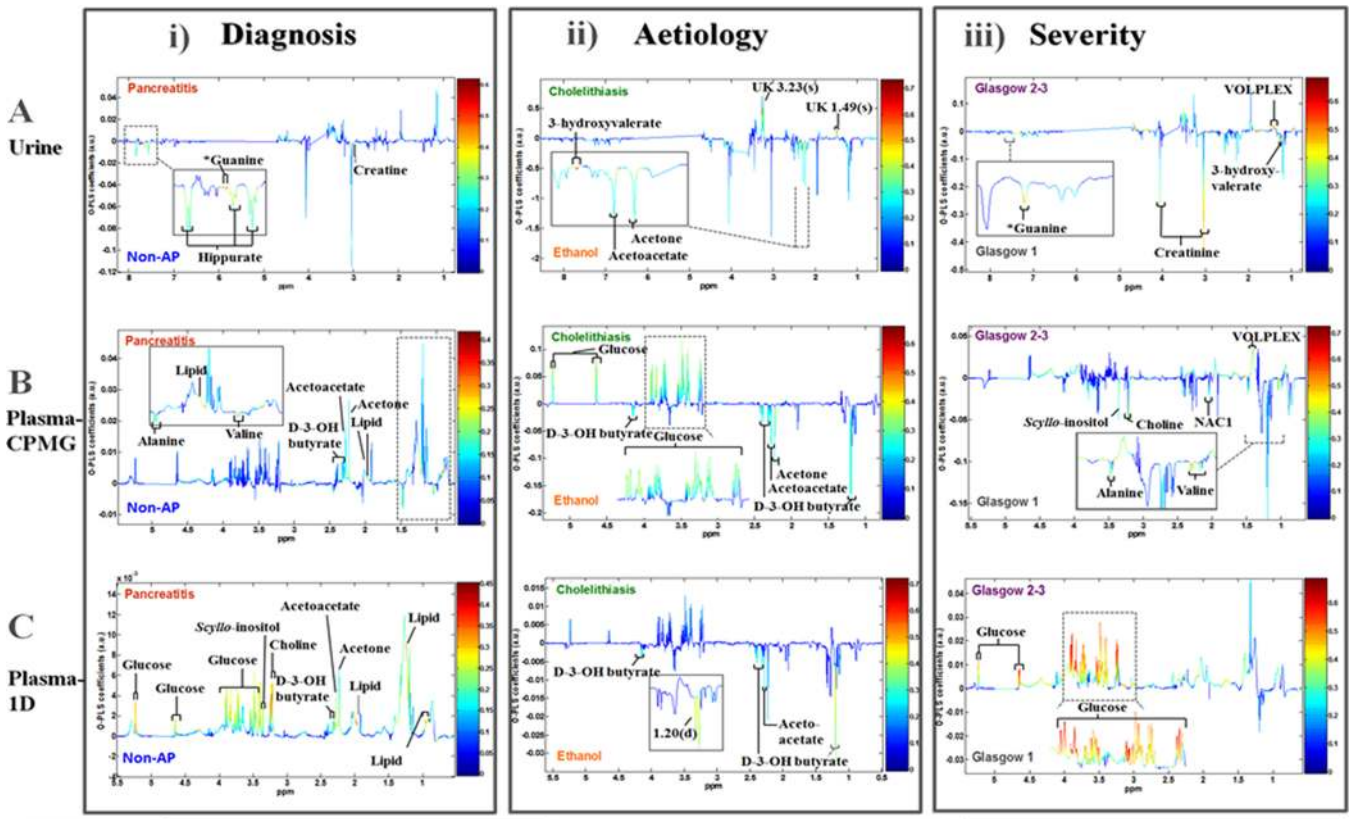

	Diagnosis		Aetiology		Severity	
	R^2	Q^2	R^2	Q^2	R^2	Q^2
Urine	0.84	0.48	0.76	0.47	0.88	0.43
CPMG	0.89	0.34	0.89*	-0.03*	0.96	0.26
1D-Plasma	0.60	0.19	0.51*	-0.33*	0.92	0.18

Figure 4. OPLS-DA coefficient plots, peak signals related to the discrimination between (i) diagnostic classes: signals indicating higher concentration in AP group (upward) versus non-AP group (downward); (ii) comparison of the main causes of pancreatitis disease: cholelithiasis (signals oriented upward) versus alcohol consumption (downward); and (iii) severity of the disease based on Glasgow score: Glasgow score 1 (upward signals) versus Glasgow score 2 and 3 (downward). The color indicates the significance of the signal association with class: the hotter the color the higher the correlation with class. All comparisons for (A) urine, (B) plasma-CPMG, and (C) 1-D-plasma used one correlated component, 1 orthogonal component in matrix X, and 0 in class Y. Key: *, the value for the first component only, unit variance scaling; two principal components.

(Figure 7). Urinary concentrations of metabolites such as malonate and 3-hydroxyisovalerate, identified from the OPLS-DA loadings plots, were higher in the group with colonic inflammation, while plasma concentrations of valine, leucine, choline, lactate, and lipids were higher in the cholelithiasis group along with urinary 3-indole acetate. These discriminant metabolites are summarized in Table 5.

DISCUSSION

The complex mechanism of AP and its associated SIRS have yet to be fully elucidated, and there is an unmet clinical need for robust diagnostic and prognostic biomarkers.[32]

Diagnosis of AP

Multivariate analysis of both urinary and plasma ^{1}H NMR spectra was able to accurately stratify patients presenting with acute abdominal pain in a clinical setting into those with AP and those with other heterogeneous causes of abdominal pain (Figure 3(i)). Urine provided a stronger predictor of AP diagnosis (ROC curve data, AUC = 0.91, Figure 6A) than plasma (ROC curve data AUC = 0.87, Figure 6B). The top five signals discriminating the AP and non-AP group in urine and in plasma were combined, and this selected panel outperformed the models for either urine or plasma individually, built from the global profile (ROC curve data AUC = 0.96, Figure 6C) observed even for the cross-validated OPLS-DA plot.

AP is associated with a disruption in glucose metabolism caused by the severe stress response, SIRS, and the resulting insulin resistance and altered pancreatic function. Insulin resistance activates secondary metabolic pathways with accelerated adipose tissue triglyceride hydrolysis causing increased ketogenesis and ketoacids visible in blood and urine. Severe vomiting, anorexia, dehydration, and alcohol use can also cause high levels of ketone bodies (acetone, D-3-hydroxybutyrate, and acetoacetic acid), which are excreted in urine (Table 2). This is supported by previous work that has found that fasting blood glucose and insulin levels are higher in AP patients than in non-AP group.[41] A striking observation was the presence of nonesterified fatty acids (NEFAs) in the plasma of patients with AP or severe illness, as governed by the APACHE II score (Figure 2). Changes in the lipid profile in our study (high levels of low-density lipoprotein [LDL; 0.86,

dx.doi.org/10.1021/pr500161w | J. Proteome Res. XXXX, XXX, XXX−XXX

Table 2. Statistically Significant Metabolites and Their Corresponding Chemical Shifts for the Diagnosis of AP (AP group vs non-AP group)

metabolite	chemical shifts (ppm) with multiplicities	AP vs non-AP group	model	driver (δ)	correl. (r)	p value
hippurate	3.96(d); 7.54(t); 7.64(t); 7.84(d)	↓	urine	7.64	−0.584	0.001
creatine	3.02(s); 3.92(s)	↓	urine	3.02	−0.508	0.004
valine	0.98(d); 1.04(d); 2.26(m); 3.60(d)	↓	CPMG	1.03	−0.356	0.033
alanine	1.47(d); 3.77(q)	↓	CPMG	1.47	−0.411	0.013
lipid CH_3CH_2	0.93(m)	↑	CPMG	0.91	0.619	0.000
			1-D-plasma		0.611	0.000
lipid $(CH_2)_n$	1.25(m)	↑	CPMG	1.245	0.420	0.011
			1-D-plasma		0.540	0.001
lipid $CH_2CH{=}CH$	1.97(m)	↑	CPMG	1.97	0.522	0.001
			1-D-plasma		0.635	0.000
choline	3.21(s)	↑	1-D-plasma	3.22	0.548	0.001
acetone	2.22(s)	↑	CPMG	2.23	0.338	0.043
			1-D-plasma		0.370	0.026
D-3-hydroxybutyrate	1.20(d); 2.31(dd); 2.41(dd); 4.16(dt)	↑	CPMG	1.19	0.347	0.038
			1-D-plasma		0.428	0.009
acetoacetic acid	2.27(s); 3.43(s)	↑	CPMG	2.28	0.326	0.052
			1-D-plasma		0.411	0.013
glucose	3.244(dd); 3.402(m); 3.49(m); 3.535(dd); 3.728(m); 3.833(m); 3.898(dd); 4.647(d); 5.233(d)	↑	1-D-plasma	5.23	0.538	0.001
scyllo-inositol	3.36(s)	↑	1-D-plasma	3.36	0.469	0.004
*guanine	7.68(s)	↓	urine	7.67	−0.535	0.002
**scyllo*-inositol	3.36(s)	↑	CPMG	3.355	0.569	0.021
*guanine	7.68(s)	↑	urine	7.679	0.657	0.015
unknown	2.83(s)	↑	urine	2.834	0.624	0.023

[a]Significance of the Pearson correlation coefficient (r) is given along with the p value for the specific driver (δ).

Table 3. Statistically Significant Metabolites and Their Corresponding Chemical Shifts for the Comparison of the AP Aetiology: Cholelithiasis vs Ethanol[a]

metabolite	chemical shifts (ppm) with multiplicities	cholelithiasis AP vs ethanol AP	matrix	driver (δ)	correl. (r)	p value
acetone	2.22(s)	↓	urine	2.24	−0.507	0.077
			CPMG plasma	2.23	−0.472	0.065
acetoacetic acid	2.27(s); 3.43(s)	↓	urine	2.29	−0.456	0.118
			CPMG plasma	3.44	−0.52	0.039
			1-D-plasma	2.28	−0.453	0.078
3-hydroxyisovalerate	1.27 (s), 2.37(s)	↓	urine	2.37	−0.851	0.000
unknown	3.23(s)	↑	urine	3.23	0.556	0.049

[a]Significance of the Pearson correlation coefficient (r) is given along with the p value for the specific driver (δ).

1.25(m)] and unsaturated lipid: $CH_2CH{=}CH$ [1.97(m)]) are consistent with known disruptions in lipid metabolism in AP, and indeed hypertriglyceridaemia is a rare but well-established cause of AP with a much more malignant phenotype.[42,43] During the acute phase response, plasma triglyceride levels rise because of increased VLDL secretion as a result of adipose tissue lipolysis, increased de novo hepatic fatty acid synthesis, and suppression of fatty acid oxidation. In cases of superimposed infection, VLDL clearance further decreases secondary to decreased lipoprotein lipase and apolipoprotein E in VLDL[44,45]. Thus, it is very likely that the striking rise in plasma VLDLs seen here relates to the generalized severity of the systemic response rather than AP-specific changes. Hyperlipidemia may also cause an elevation of plasma choline associated with triglyceride breakdown or more likely phosphatidylcholine, which, in turn, leads to the formation of fatty acids and an exacerbation of the ketonuria. In general, these changes are commonly observed in diabetes.[46]

To our knowledge, the lower plasma concentrations of alanine and valine in the AP group observed here have not been reported previously for AP, although decreased concentrations of amino acids (leucine, isoleucine, valine, and alanine) have been found in both rodent[47] and human[48] models of CP, and lower levels of valine have been found in CP patients when compared with acute necrotizing pancreatitis.[49] It is relevant that both alanine and valine are components of pancreatic juice,[50] and their fall in circulating concentrations may be related to an exocrine pancreatic insufficiency that is characteristic of severe AP.

A significant anticorrelation was found for hippurate and AP, which was only partially accounted for by antibiotic usage (Figure 5 and Supplemental Table 1, SI). Because hippurate, a well-established gut microbial cometabolite and biomarker of hepatic reserve,[38] was not significantly associated with antibiotic usage, this supports the theory that SIRS in AP leads to mesenteric hypoperfusion,[51] which in turn may disrupt the gut luminal environment and subsequently gut microbial function.

dx.doi.org/10.1021/pr500161w | J. Proteome Res. XXXX, XXX, XXX−XXX

Table 4. Statistically Significant Metabolites and Their Corresponding Chemical Shifts for the Comparison of the Severity of the Pancreatitis between Mild AP (Glasgow 1) vs Moderate to Severe AP (Glasgow 2−3)

metabolite	chemical shifts (ppm) with multiplicities	Glasgow score 1 vs 2−3 in AP group	matrix	driver (δ)	correl. (r)	p value
lipid CH_3CH_2	0.93(m)	↓	1-D-plasma	0.925	−0.565	0.023
			CPMG plasma	0.925	−0.560	0.024
lipid $CH_2C{=}C$	2.00 (m)	↓	1-D-plasma	2.026	−0.554	0.026
creatinine	3.05(s); 4.05(s)	↑	urine	3.046	0.655	0.015
malonic acid	3.12(s)	↑	urine	3.119	0.625	0.023
choline $(CH_3)_3{-}N$	3.21(s)	↑	CPMG plasma	3.214	0.600	0.014
valine	0.98(d); 1.03(d); 2.26(m); 3.60(d)	↑	CPMG plasma	1.044	0.690	0.003
isoleucine	0.94(t); 1.01(d); 1.26(m); 1.48(m); 1.98(m); 3.68(m)	↑	CPMG plasma	1.012	0.550	0.027
alanine	1.47(d); 3.77(q)	↑	CPMG plasma	1.479	0.542	0.03
acetyl signals from α1-acid glycoprotein (NAC1)	2.04(s)	↑	CPMG plasma	2.037	0.557	0.025
$\alpha + \beta$ D-glucose	3.244(dd); 3.402(m); 3.49(m); 3.535(dd); 3.728(m); 3.833(m); 3.898(dd); 4.647(d); 5.233(d)	↓	1-D-plasma	3.244	−0.723	0.002
**scyllo*-inositol	3.36(s)	↑	CPMG plasma	3.355	0.569	0.021
*guanine	7.68(s)	↑	urine	7.679	0.657	0.015
unknown	2.83(s)	↑	urine	2.834	0.624	0.023

[a]Significance of the Pearson correlation coefficient (r) is given along with the p value for the specific driver (δ); *tentative assignment.

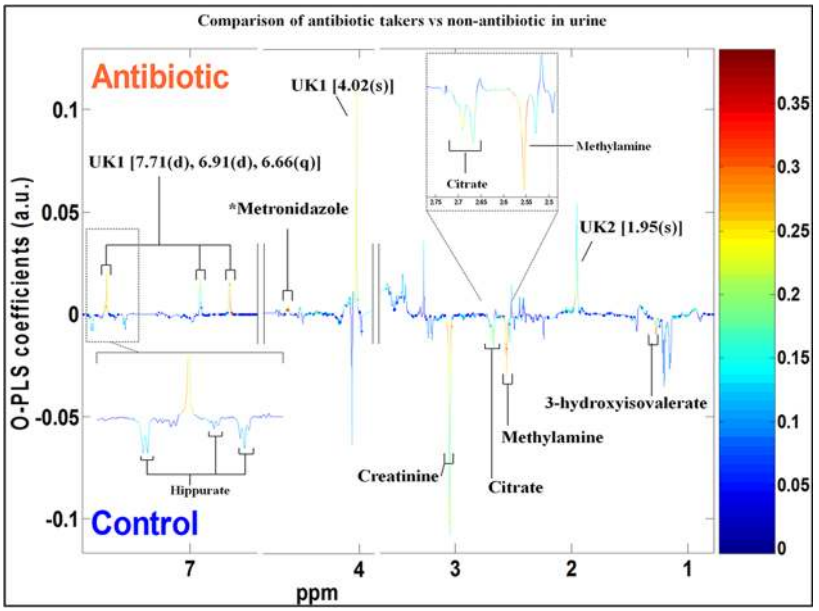

Figure 5. OPLS-DA coefficients plot. Peak signals related to the discrimination between antibiotic consumers (top) group vs nonantibiotic takers (bottom). Models were created using unit variance scaling, $R^2 = 0.85$ and $Q^2 = 0.47$. ●, Antibiotic takers (n = 10 [5non-AP/5AP]); ■, nonantibiotic samples (n = 21 [12non-AP/9AP]).

This also fits with the theory of gut bacterial translocation in AP,[52] which is thought to explain the high rates of enteric bacteria identified in cases of pancreatic necrosis and sepsis. However, we are unable to exclude the possibility that altered hepatic glycine conjugation of benzoyl CoA may also explain this finding.

Etiology of AP Caused by Alcohol Consumption and Cholelithiasis

The two causes of AP in this series were alcohol (9/15) and cholelithiasis, which is representative of the epidemiology of the condition. Metabolites such as acetone, acetoacetate, and 3-hydroxyisovalerate (Table 3) were predictive for alcohol-induced AP. It is well established that alcohol consumption influences the regulation of key pathways such as gluconeogenesis. Ketone bodies are products of the oxidative pathway of alcohol metabolism[53] and are thus concordant with this observation discriminating the alcohol-induced AP patients, although because there were no dietary records for the patients, the possibility that anorexia, associated with severe abdominal pain, may have been systematically different between the groups and therefore a contributor to the ketone body profile.

AP Severity Based on the Glasgow Severity Score

The raw NMR spectra from severely unwell AP patients were highly variable in structure compared with control patients (Figures 1 and 2). However, these data provide a strong metabolic phenotype of the severity of illness and a clear metabolic description of AP disease severity. AP patients with moderate to severe AP disease (Glasgow 2−3) had higher levels of glucose and reduced plasma relative concentrations of alanine, valine, choline, the acetyl signal from α1-acid

dx.doi.org/10.1021/pr500161w | J. Proteome Res. XXXX, XXX, XXX−XXX

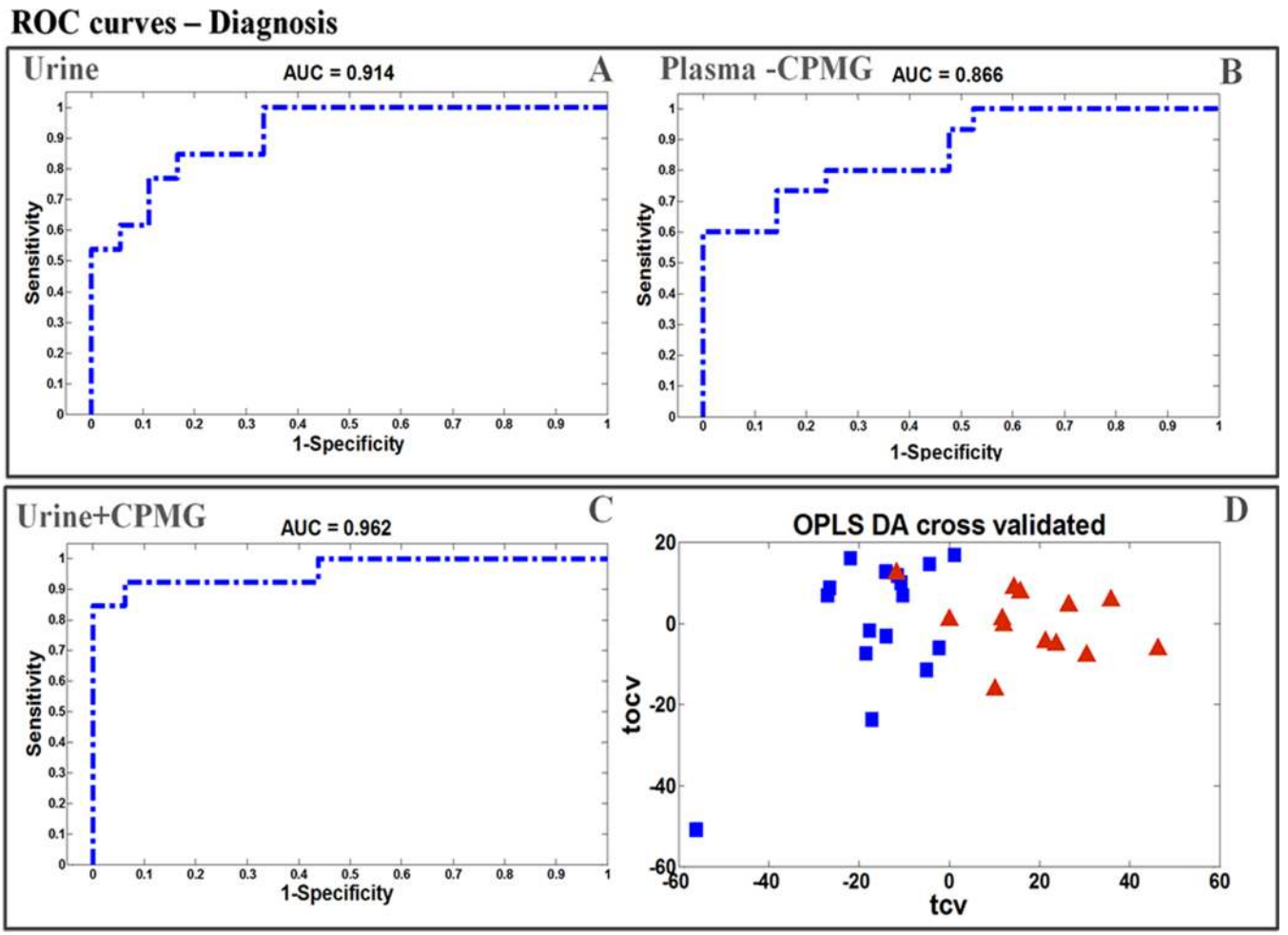

Figure 6. ROC plot for (A) urinary data set (n = 31 [18non-AP/13AP]) and (B) plasma-CPMG spin−echo (n = 36 [21non-AP/15AP]). (C) Combination of 10 metabolites in total from urine (guanine at 7.67(s), hippurate at 7.54(t), 7.64(t), 7.84(d), creatine at 3.02(s) and unknown metabolites at 2.73(s), and 4.55(d), and CPMG plasma (valine at 1.04(d), alanine at 1.47 (d), and lipid compounds at 0.91(m), 1.25(m), and 1.97(m)); OPLS-DA was cross-validated from the previous ROC curve (R^2 = 0.76, Q^2 = 0.59, n = 29 [16non-AP/13AP]).

glycoprotein (NAC1), and urinary creatinine (Table 4). As previously described, this combined cohort of metabolic changes is suggestive of insulin resistance[54] and probable failure of pancreatic function, with the NAC1 most likely reflecting generalized inflammation.[55]

Differentiation of Metabolic Phenotypes within the Non-AP Group

It was possible to distinguish between subclasses of the non-AP group (Figure 7 and Table 5) using the metabolic profiles, which is of importance to the clinical setting. Patients with cholelithiasis demonstrated higher concentrations of lactate, choline, valine, leucine, and lipids in the plasma and increased urinary indoleacetate levels. Indoleacetate is a metabolite produced from tryptophan by several intestinal bacteria. High levels of indoleacetate have typically been related to gastrointestinal cancer and hepato-biliary tract cancer, and high concentrations have been observed in patients with cirrhosis, diabetes, and cholelithiasis occasionally.[56] Our data are in keeping with independent studies that suggest that low plasma choline concentrations are associated with cholelithiasis and colonic inflammation.[57,58] The negative correlation of branched-chain amino acids (valine and leucine) with the colonic inflammation group is also consistent with data from inflammatory bowel disease patients.[58]

This study has several limitations, which must be accounted for when interpreting the data. The numbers of patients was relatively small and the study was not powered for mortality. A larger numbers of patients with greater severity of illness are required to build more accurate prognostic models that are not based on surrogate markers of disease severity and to explore the power of global metabolic profiling to distinguish between rarer causes of AP (e.g., viral, drug-induced, or hypertriglyceridaemia). Also, males were statistically over-represented in the AP group, although this is a reflection of the epidemiology of the disease. Nevertheless, we have demonstrated a convincing metabolic phenotype for the diagnosis, etiology, and severity of AP. It is likely that much of the diagnostic power of this model relates to the significant severity of illness encountered in patients when compared with generic peritonitic patients, as found in the variation between the APACHE II scores and the hospital LOS (Table 1). The lipid signature appears to be extremely important in making this differentiation, and the overall result of this scoping study suggests that a global metabolic profiling approach has significant potential for the early detection and diagnosis of critically unwell patients.

dx.doi.org/10.1021/pr500161w | J. Proteome Res. XXXX, XXX, XXX−XXX

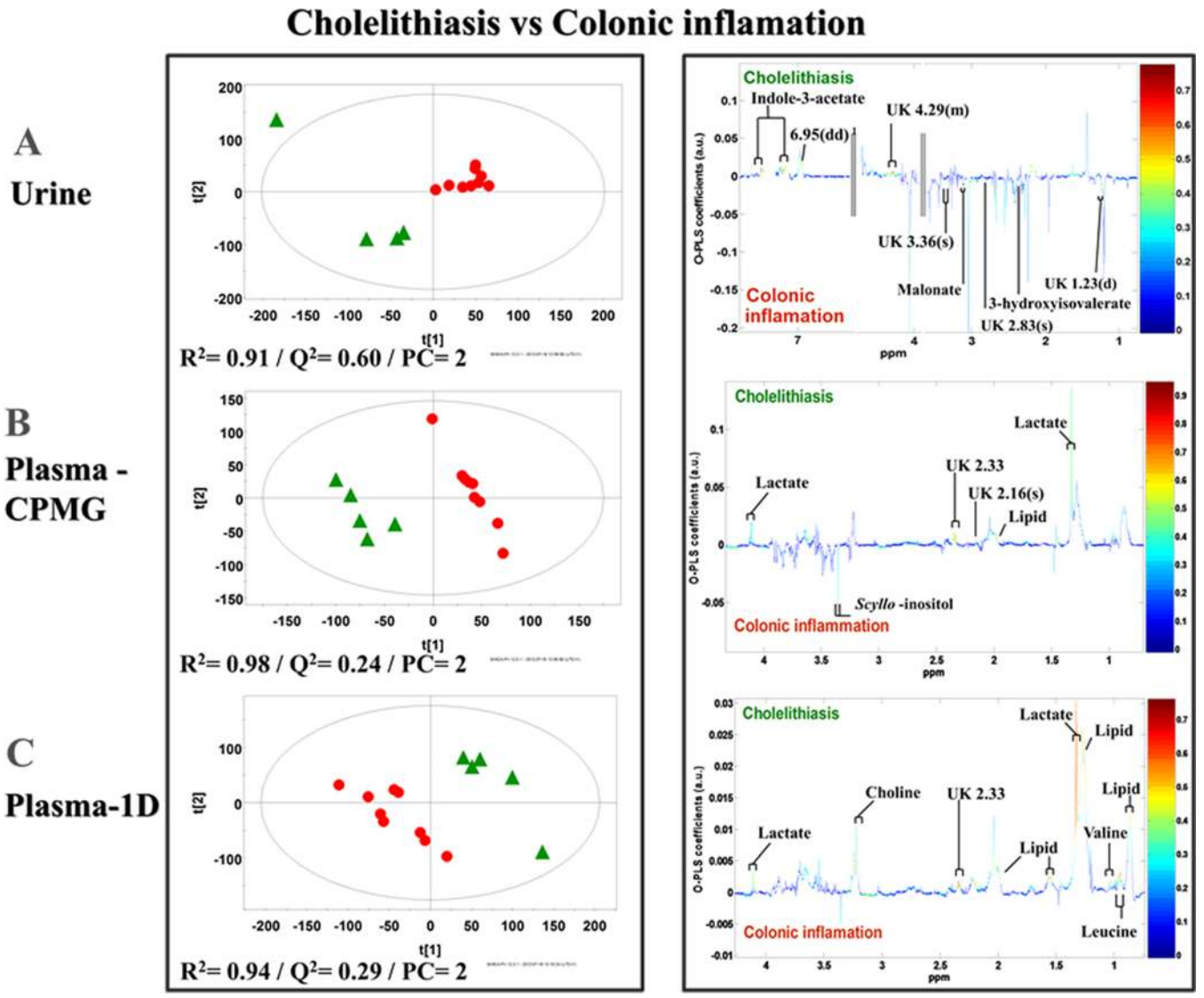

Figure 7. PLS-DA scores plot for (A) urine, (B) plasma-CPMG spin−echo, and (C) 1-D-plasma for patients comparing cholelithiasis versus colonic inflammation (including diverticulitis, appendicitis, Crohn's disease, and ischemia) within the non-AP group (Table 1). (B) OPLS-DA loading plot for the discrimination between patients with cholelithiasis (upward facing signals) versus patients with colonic inflammation (downward). The model was built using unit variance scaling. R^2 and Q^2 values signify variance explained and predictivity of the model, respectively. △, cholelithiasis patients (A-B-Cn = 5); ●, patients with colonic inflammation (A-B-Cn = 9).

Table 5. Statistically Significant Metabolites and Their Corresponding Chemical Shifts in the Non-AP Patient Comparison: Cholelithiasis versus Colonic Inflammation[a]

metabolite	chemical shifts (ppm) with multiplicities	colonic inflammation vs cholelithiasis	matrix	driver (δ)	correl. (r)	p value
indole-3-acetate	3.65(s); 7.15(dd); 7.24(m); 7.50(d); 7.62(d)	↓	urine	7.50	−0.711	0.004
lactate	1.33(d); 4.11(q)	↓	CPMG plasma	1.33	−0.623	0.017
			1-D-plasma	1.32	−0.777	0.001
lipid (mainly VLDL)	0.87(t)	↓	1-D-plasma	0.87	−0.635	0.015
lipid (mainly LDL)	1.25(m)	↓	1-D-plasma	1.26	−0.702	0.005
lipid (mainly VLDL)	1.56(m)	↓	1-D-plasma	1.56	−0.628	0.016
lipid $CH_2CH{=}CH$	2.00(m)	↓	1-D-plasma	2.00	−0.604	0.022
leucine	0.95(t); 1.7(m); 3.72(m)	↓	1-D-plasma	0.95	−0.771	0.001
valine	0.98(d); 1.03(d); 2.26(m); 3.60(d)	↓	1-D-plasma	1.03	−0.584	0.028
malonic acid	3.12(s)	↑	urine	3.12	0.652	0.012
choline	3.21(s)	↓	1-D-plasma	3.22	−0.541	0.046
3-hydroxyvalerate	1.27 (s), 2.37(s)	↑	urine	2.37	0.656	0.011

[a]Significance of the Pearson correlation coefficient (r) is given along with the p value for the specific driver (δ).

dx.doi.org/10.1021/pr500161w | J. Proteome Res. XXXX, XXX, XXX−XXX

CONCLUSIONS

We have demonstrated a diagnostic and prognostic phenotype of AP that reflects the severity of the systemic inflammation. In particular, we found the plasma lipid signature to be important in the clinical diagnosis of AP alongside valine, alanine, and hippurate, differentiating AP from other common causes of abdominal pain. Information about drug metabolism, dietary influences on disease biology, and the possible contribution of the gut microbiota in the disease mechanism was also obtained using a metabonomic framework. Finally, this work has shown clinical utility of metabolic phenotyping approaches in the diagnosis of acute abdominal pain and in the critical care setting. Further work is required in much larger patient cohorts to further validate these findings and to refine the metabolic signature attributable to underlying etiologies.

ASSOCIATED CONTENT

Supporting Information

STOCSY plot derived from the correlation matrix calculated between the data point at the peak of 3-hydroxyisovalerate at δ 2.37 and all other data points. ^{1}H-NMR spectra from a patient with acute on chronic alcoholic pancreatitis. Pearson correlation structure obtained after selecting driver peak from mannitol [δ 3.805, (5-CH)] in the 1-D NMR profile and applying a p = 0.05 significance criterion. 600 MHz CPMG spectra (δ −0.0 to 4.7) of serum plasma. STOCSY plot derived from the correlation matrix calculated between the data point at the peak of acetaminophen at δ 2.16 and all other data points. Scores plot of the first versus second component of the principal component analysis using the most discriminant metabolites from urine and CPMG. Permutation test plot from PLS-DA using the most discriminant metabolites from urine and CPMG matrices. Statistically significant metabolites and their corresponding chemical shifts in the antibiotic consumers group versus controls. Biochemical clinical parameters a comparison between AP and non-AP group. This material is available free of charge via the Internet at http://pubs.acs.org.

AUTHOR INFORMATION

Corresponding Authors

*J.M.K.: Tel: +44 (0) 79 8934 4238. E-mail: j.kinross@imperial.ac.uk.
*E.H.: Tel: +44 (0) 20 7594 3220. Fax: +44 (0) 20 7594 3226. E-mail: elaine.holmes@imperial.ac.uk.

Notes

The authors declare no competing financial interest.

ACKNOWLEDGMENTS

The research was supported by the National Institute for Health Research (NIHR) Biomedical Research Centre based at Imperial College Healthcare NHS Trust and Imperial College London. The views expressed are those of the author(s) and not necessarily those of the NHS, the NIHR, or the Department of Health. J.M.K. acknowledges the funding from the Academy of Medical Sciences. CEMBIO authors acknowledge the funding to Spanish Ministry of Economy and Competitiveness (MEC) grant CTQ2011-23562, and A.V. acknowledges her fellowship to EADS CASA and Santander bank for the mobility grant.

ABBREVIATIONS

AP, acute pancreatitis; SIRS, systemic inflammatory response syndrome; USS, abdominal ultrasound imaging; CT, computed tomography; ^{1}H NMR, proton nuclear magnetic resonance; ERCP, endoscopic retrograde cholangio pancreatography; FID, free induction decay; CPMG, Carr−Purcell−Meiboom−Gill spin−eco; TSP, trimethylsilypropionate; PCA, principal component analysis; PLSDA, partial least-squares discriminant analysis; OPLS-DA, orthogonal-PLSDA; STOCSY, statistical total correlation spectroscopy; TOCSY, total correlation spectroscopy; HMQC, heteronuclear multiple-quantum correlation; HSQC, heteronuclear single-quantum correlation; APACHE II, acute physiology and chronic health evaluation II; NSAID, nonsteroidal anti-inflammatory drug; TPR, true-positive rates; FPR, false-positive rates; ROC, receiver operating characteristic; AUC, area under the ROC curve; VLDL, very-low-density lipoprotein; LDL, low-density lipoprotein; CP, chronic pancreatitis; NAC1, acetyl signal from α1-acid glycoprotein[59]; MS, mass spectrometry; PAG, phenylacetylglutamine

REFERENCES

(1) Baddeley, R. N.; Skipworth, J. R.; Pereira, S. P. Acute pancreatitis. *Medicine* **2010**, *39* (2), 108−115.
(2) Fan, B.-G.; Andrén-Sandberg, Å. Acute pancreatitis. *N. Am. J. Med. Sci.* **2010**, *2* (5), 211−214.
(3) Treacy, J.; Williams, A.; Bais, R.; Willson, K.; Worthley, C.; Reece, J.; Bessell, J.; Thomas, D. Evaluation of amylase and lipase in the diagnosis of acute pancreatitis. *ANZ. J. Surg.* **2001**, *71* (10), 577−582.
(4) Xiao, B.; Zhang, X. M. Magnetic resonance imaging for acute pancreatitis. *World J. Radiol* **2010**, *2* (8), 298−308.
(5) Lempinen, M.; Puolakkainen, P.; Kemppainen, E. Clinical value of severity markers in acute pancreatitis. *Scand. J. Surg.* **2005**, *94* (2), 118−123.
(6) Cerrudo, J. J.; Roselló, A. M.; Yañez, A. P.; Jiménez, I. S.; Orihuela, J. A. F. Urgent vascular complications in acute pancreatitis. *Cir. Esp.* **2011**, *90* (2), 134−136.
(7) Raimondi, S.; Lowenfels, A. B.; Morselli-Labate, A. M.; Maisonneuve, P.; Pezzilli, R. Pancreatic cancer in chronic pancreatitis; aetiology, incidence, and early detection. *Best Pract. Res., Clin. Gastroenterol.* **2010**, *24* (3), 349−358.
(8) Vonlaufen, A.; Wilson, J. S.; Apte, M. V. Molecular mechanisms of pancreatitis: current opinion. *J. Gastroenterol. Hepatol.* **2008**, *23* (9), 1339−1348.
(9) Chiang, D. T.; Anozie, A.; Fleming, W. R.; Kiroff, G. K. Comparative study on acute pancreatitis management. *ANZ. J. Surg.* **2004**, *74* (4), 218−221.
(10) Keller, J.; Layer, P. Idiopathic chronic pancreatitis. *Best Pract. Res., Clin. Gastroenterol.* **2008**, *22* (1), 105−113.
(11) Bezmarević, M.; Kostić, Z.; Jovanović, M.; Micković, S.; Mirković, D.; Soldatović, I.; Trifunović, B.; Pejović, J.; Vujanić, S. Procalcitonin and BISAP score versus C-reactive protein and APACHE II score in early assessment of severity and outcome of acute pancreatitis. *Vojnosanit. Pregl.* **2012**, *69* (5), 425−31.
(12) Sekimoto, M.; Takada, T.; Kawarada, Y.; Hirata, K.; Mayumi, T.; Yoshida, M.; Hirota, M.; Kimura, Y.; Takeda, K.; Isaji, S.; Koizumi, M.; Otsuki, M.; Matsuno, S. JPN, JPN Guidelines for the management of acute pancreatitis: epidemiology, etiology, natural history, and outcome predictors in acute pancreatitis. *J. Hepato-Biliary-Pancreatic Surg.* **2006**, *13* (1), 10−24.
(13) Spanier, B. W.; Dijkgraaf, M. G.; Bruno, M. J. Epidemiology, aetiology and outcome of acute and chronic pancreatitis: An update. *Best Pract. Res., Clin. Gastroenterol.* **2008**, *22* (1), 45−63.

(14) Nicholson, J. K.; Wilson, I. D. Opinion: understanding 'global' systems biology: metabonomics and the continuum of metabolism. *Nat. Rev. Drug Discovery* **2003**, *2* (8), 668−676.
(15) Lindon, J. C.; Nicholson, J. K.; Holmes, E.; Everett, J. R. Metabonomics: Metabolic Processes Studied by NMR Spectroscopy of Biofluids. *Concepts Magn. Reson.* **2000**, *12* (5), 289−320.
(16) Nicholson, J. K.; Holmes, E.; Kinross, J. M.; Darzi, A. W.; Takats, Z.; Lindon, J. C. Metabolic phenotyping in clinical and surgical environments. *Nature* **2012**, *491* (7424), 384−392.
(17) Lenz, E. M.; Wilson, I. D. Analytical strategies in metabonomics. *J. Proteome Res.* **2007**, *6* (2), 443−458.
(18) Nicholson, J. K.; Connelly, J.; Lindon, J. C.; Holmes, E. Metabonomics: a platform for studying drug toxicity and gene function. *Nat. Rev. Drug Discovery* **2002**, *1* (2), 153−161.
(19) Lindon, J. C.; Nicholson, J. K. Analytical technologies for metabonomics and metabolomics, and multi-omic information recovery. *TrAC, Trends Anal. Chem.* **2008**, *27* (3), 194−204.
(20) Lusczek, E. R.; Paulo, J. A.; Saltzman, J. R.; Kadiyala, V.; Banks, P. A.; Beilman, G.; Conwell, D. L. Urinary ^{1}H-NMR metabolomics can distinguish pancreatitis patients from healthy controls. *J. Pancreas* **2013**, *14* (2), 161−170.
(21) UK guidelines for the management of acute pancreatitis. *Gut* **2005**, *54* Suppl 3, iii1−9.
(22) Braganza, J. M.; Lee, S. H.; McCloy, R. F.; McMahon, M. J. Chronic pancreatitis. *Lancet* **2011**, *377* (9772), 1184−1197.
(23) Beckonert, O.; Keun, H. C.; Ebbels, T. M.; Bundy, J.; Holmes, E.; Lindon, J. C.; Nicholson, J. K. Metabolic profiling, metabolomic and metabonomic procedures for NMR spectroscopy of urine, plasma, serum and tissue extracts. *Nat. Protoc.* **2007**, *2* (11), 2692−2703.
(24) Veselkov, K. A.; Lindon, J. C.; Ebbels, T. M.; Crockford, D.; Volynkin, V. V.; Holmes, E.; Davies, D. B.; Nicholson, J. K. Recursive segment-wise peak alignment of biological ^{1}H NMR spectra for improved metabolic biomarker recovery. *Anal. Chem.* **2009**, *81* (1), 56−66.
(25) Dieterle, F.; Ross, A.; Schlotterbeck, G.; Senn, H. Probabilistic quotient normalization as robust method to account for dilution of complex biological mixtures. Application in ^{1}H NMR metabonomics. *Anal. Chem.* **2006**, *78* (13), 4281−4290.
(26) Eriksson, I.; Johansson, E.; Kettaneh-Wold, N.; Wold, S. *Multi- and Megavariate Data Analysis and Applications*; Umetrics: Umea, Sweden, 2001; p 533.
(27) Bylesjö, M.; Rantalainen, M.; Cloarec, O.; Nicholson, J.; Holmes, E.; Trygg, J. OPLS discriminant analysis: combining the strengths of PLS-DA and SIMCA classification. *J. Chemom.* **2006**, *20*, 341−351.
(28) Cloarec, O.; Dumas, M. E.; Trygg, J.; Craig, A.; Barton, R. H.; Lindon, J. C.; Nicholson, J. K.; Holmes, E. Evaluation of the orthogonal projection on latent structure model limitations caused by chemical shift variability and improved visualization of biomarker changes in ^{1}H NMR spectroscopic metabonomic studies. *Anal. Chem.* **2005**, *77* (2), 517−526.
(29) Cloarec, O.; Dumas, M. E.; Craig, A.; Barton, R. H.; Trygg, J.; Hudson, J.; Blancher, C.; Gauguier, D.; Lindon, J. C.; Holmes, E.; Nicholson, J. Statistical total correlation spectroscopy: an exploratory approach for latent biomarker identification from metabolic ^{1}H NMR data sets. *Anal. Chem.* **2005**, *77* (5), 1282−1289.
(30) Wishart, D. S.; Tzur, D.; Knox, C.; Eisner, R.; Guo, A. C.; Young, N.; Cheng, D.; Jewell, K.; Arndt, D.; Sawhney, S.; Fung, C.; Nikolai, L.; Lewis, M.; Coutouly, M. A.; Forsythe, I.; Tang, P.; Shrivastava, S.; Jeroncic, K.; Stothard, P.; Amegbey, G.; Block, D.; Hau, D. D.; Wagner, J.; Miniaci, J.; Clements, M.; Gebremedhin, M.; Guo, N.; Zhang, Y.; Duggan, G. E.; Macinnis, G. D.; Weljie, A. M.; Dowlatabadi, R.; Bamforth, F.; Clive, D.; Greiner, R.; Li, L.; Marrie, T.; Sykes, B. D.; Vogel, H. J.; Querengesser, L. HMDB: the Human Metabolome Database. *Nucleic Acids Res.* **2007**, *35* (Database issue), D521−D526.
(31) Robinette, S. L.; Zhang, F.; Bruschweiler-Li, L.; Bruschweiler, R. Web server based complex mixture analysis by NMR. *Anal. Chem.* **2008**, *80* (10), 3606−11.
(32) Cartwright, S. L.; Knudson, M. P. Evaluation of acute abdominal pain in adults. *Am. Fam. Physician* **2008**, *77* (7), 971−8.
(33) Bales, J. R.; Sadler, P. J.; Nicholson, J. K.; Timbrell, J. A. Urinary excretion of acetaminophen and its metabolites as studied by proton NMR spectroscopy. *Clin. Chem.* **1984**, *30* (10), 1631−1636.
(34) Spraul, M.; Hofmann, M.; Dvortsak, P.; Nicholson, J. K.; Wilson, I. D. High-performance liquid chromatography coupled to high-field proton nuclear magnetic resonance spectroscopy: application to the urinary metabolites of ibuprofen. *Anal. Chem.* **1993**, *65* (4), 327−330.
(35) Garcia-Perez, I.; Couto Alves, A.; Angulo, S.; Li, J. V.; Utzinger, J.; Ebbels, T. M.; Legido-Quigley, C.; Nicholson, J. K.; Holmes, E.; Barbas, C. Bidirectional correlation of NMR and capillary electrophoresis fingerprints: a new approach to investigating Schistosoma mansoni infection in a mouse model. *Anal. Chem.* **2010**, *82* (1), 203−210.
(36) Gohel, M. C.; Jogani, P. D. A review of co-processed directly compressible excipients. *J. Pharm. Pharm. Sci.* **2005**, *8* (1), 76−93.
(37) Zheng, X.; Xie, G.; Zhao, A.; Zhao, L.; Yao, C.; Chiu, N. H.; Zhou, Z.; Bao, Y.; Jia, W.; Nicholson, J. K. The footprints of gut microbial-mammalian co-metabolism. *J. Proteome Res.* **2011**, *10* (12), 5512−5522.
(38) Lees, H. J.; Swann, J. R.; Wilson, I. D.; Nicholson, J. K.; Holmes, E., Hippurate: The Natural History of a Mammalian-Microbial Cometabolite. *J. Proteome Res.* **2013**.
(39) Coleman, M. D.; Norton, R. S. Observation of drug metabolites and endogenous compounds in human urine by 1H nuclear magnetic resonance spectroscopy. *Xenobiotica* **1986**, *16* (1), 69−77.
(40) Kinross, J. M.; Darzi, A. W.; Nicholson, J. K. Gut microbiome-host interactions in health and disease. *Genome Med.* **2011**, *3* (3), 14.
(41) Wu, D.; Xu, Y.; Zeng, Y.; Wang, X. Endocrine pancreatic function changes after acute pancreatitis. *Pancreas* **2011**, *40* (7), 1006−1011.
(42) Stefanutti, C.; Labbadia, G.; Morozzi, C. Severe hypertriglyceridemia-related acute pancreatitis. *Ther. Apheresis Dial.* **2013**, *17* (2), 130−137.
(43) Serpytis, M.; Karosas, V.; Tamosauskas, R.; Dementaviciene, J.; Strupas, K.; Sileikis, A.; Sipylaite, J. Hypertriglyceridemia-induced acute pancreatitis in pregnancy. *J. Pancreas* **2012**, *13* (6), 677−680.
(44) Khovidhunkit, W.; Kim, M. S.; Memon, R. A.; Shigenaga, J. K.; Moser, A. H.; Feingold, K. R.; Grunfeld, C. Effects of infection and inflammation on lipid and lipoprotein metabolism: mechanisms and consequences to the host. *J. Lipid Res.* **2004**, *45* (7), 1169−1196.
(45) Bartolomé, N.; Aspichueta, P.; Martínez, M. J.; Vázquez-Chantada, M.; Martínez-Chantar, M. L.; Ochoa, B.; Chico, Y. Biphasic adaptative responses in VLDL metabolism and lipoprotein homeostasis during Gram-negative endotoxemia. *Innate Immun.* **2012**, *18* (1), 89−99.
(46) Solanki, N. S.; Barreto, S. G.; Saccone, G. T. Acute pancreatitis due to diabetes: the role of hyperglycaemia and insulin resistance. *Pancreatology* **2012**, *12* (3), 234−239.
(47) Fang, F.; He, X.; Deng, H.; Chen, Q.; Lu, J.; Spraul, M.; Yu, Y. Discrimination of metabolic profiles of pancreatic cancer from chronic pancreatitis by high-resolution magic angle spinning 1H nuclear magnetic resonance and principal components analysis. *Cancer Sci.* **2007**, *98* (11), 1678−1682.
(48) Adrych, K.; Smoczynski, M.; Stojek, M.; Sledzinski, T.; Slominska, E.; Goyke, E.; Smolenski, R. T.; Swierczynski, J. Decreased serum essential and aromatic amino acids in patients with chronic pancreatitis. *World J. Gastroenterol* **2010**, *16* (35), 4422−4427.
(49) Ma, C.; Tian, B.; Wang, J.; Yang, G. J.; Pan, C. S.; Lu, J. P. Metabolic characteristics of acute necrotizing pancreatitis and chronic pancreatitis. *Mol. Med. Rep.* **2012**, *6* (1), 57−62.
(50) Wang, J.; Ma, C.; Liao, Z.; Tian, B.; Lu, J. P. Study on chronic pancreatitis and pancreatic cancer using MRS and pancreatic juice samples. *World J. Gastroenterol.* **2011**, *17* (16), 2126−2130.
(51) Giakoustidis, A.; Mudan, S. S.; Giakoustidis, D. Dissecting the stress activating signaling pathways in acute pancreatitis. *Hepatogastroenterology* **2010**, *57* (99−100), 653−656.

(52) Li, Q.; Wang, C.; Tang, C.; He, Q.; Li, N.; Li, J. Bacteremia in the Patients With Acute Pancreatitis as Revealed by 16S Ribosomal RNA Gene-Based Techniques. *Crit. Care Med.* **2013**, *41* (8), 1938−1950.
(53) Nicholas, P. C.; Kim, D.; Crews, F. T.; Macdonald, J. M. ^{1}H NMR-based metabolomic analysis of liver, serum, and brain following ethanol administration in rats. *Chem. Res. Toxicol.* **2008**, *21* (2), 408−420.
(54) Zuo, Y. Y.; Kang, Y.; Yin, W. H.; Wang, B.; Chen, Y. The association of mean glucose level and glucose variability with intensive care unit mortality in patients with severe acute pancreatitis. *J. Crit. Care* **2012**, *27* (2), 146−152.
(55) Billingham, M. E.; Gordon, A. H. The role of the acute phase reaction in inflammation. *Agents Actions* **1976**, *6* (1−3), 195−200.
(56) Kobori, K.; Sakakibara, H.; Maruyama, K.; Kobayashi, T.; Yamaki, T. A rapid method for determining urinary indoleacetic acid concentration and its clinical significance as the tumor-marker in the diagnosis of malignant diseases. *J. UOEH* **1983**, *5* (2), 213−220.
(57) Kelly, D. A. Intestinal failure-associated liver disease: what do we know today? *Gastroenterology* **2006**, *130* (2 Suppl 1), S70−S77.
(58) Balasubramanian, K.; Kumar, S.; Singh, R. R.; Sharma, U.; Ahuja, V.; Makharia, G. K.; Jagannathan, N. R. Metabolism of the colonic mucosa in patients with inflammatory bowel diseases: an in vitro proton magnetic resonance spectroscopy study. *Magn. Reson. Imaging* **2009**, *27* (1), 79−86.
(59) Bell, J. D.; Brown, J. C.; Nicholson, J. K.; Sadler, P. J. Assignment of resonances for 'acute-phase' glycoproteins in high resolution proton NMR spectra of human blood plasma. *FEBS Lett.* **1987**, *215* (2), 311−315.

■ NOTE ADDED AFTER ASAP PUBLICATION

This paper was published ASAP on October 8, 2014. The corrected version was reposted on October 10, 2014, with additional text changes, notably in the abstract and the addition of reference 59.